Ann. Physik 1 (1992) 254–269

Annalen
der Physik
© Johann Ambrosius Barth 1992

Response of finite many-electron systems beyond the time-dependent local density approximation: Application to small metal clusters

J. M. Pacheco[1]* and W. Ekardt[2]**

[1]Fritz-Haber Institut der Max-Planck Gesellschaft, Faradayweg 4–6, W-1000 Berlin 33, Germany
[2]Niels Bohr Institute, Blegdamsvej 17, DK-2100 Copenhagen Ø, Denmark

Received 24 February 1992, accepted 10 April 1992

Abstract. A linear response formalism is developed which is based on density functional theory within the local density approximation, but which is now corrected for its spurious self-interaction errors, in the way originally proposed by Perdew and Zunger for ground state calculations. The original formulation is extended to incorporate self-interaction corrections in the scrrening terms. The general formalism is then applied to the calculation of the static and dynamic response of the metal clusters $\{Na_8, Na_9^+\}$, $\{Na_{20}, Na_{21}^+\}$ and $\{Na_{40}, Na_{41}^+\}$ within the jellium model. Comparison with experimental data and with other theoretical calculations indicates that the present formalism accounts for the overall (and most of the fine) features of the photoabsorption spectrum of these systems, providing a systematic improvement with respect to previous approaches. The remaining discrepancies are rationalized in terms of the effects to be expected by correctly accounting for the discrete structure of the ionic cores.

Keywords: Atomic and molecular clusters; Excites states; Visible spectra.

1 Introduction

The special stability of small particles of alkali metals containing 8, 20, 40, . . . valence electrons was predicted by one of us [1] to be a physically observable effect associated with the closure of shells of electrons moving independently in a spherically symmetric average potential. These conjectures were based on the theoretical description of the valence electrons of these systems by means of Density Functional Theory (DFT), invoking the Local Density Approximation (LDA) for Exchange and Correlation (XC), and replacing the ionic cores by a smeared, positive, constant and spherical volume charge density of radius $R_0 = r_s \mathcal{N}^{1/3}$, r_s being the Wigner-Seitz radius of the bulk metal and $\mathcal{N}$ the total number of atoms (the so-called jellium model). A few months later, experiments carried out in Berkeley by Knight et al. [2] were published, confirming these predictions and proposing the shell model for the valence electrons of metal clusters. Mainly due to their remarkable simplicity, jellium and jellium-based models have been widely used in cluster physics since then.

As early as 1984, the Time-Dependent LDA (TDLDA), developed in 1980 in atomic physics [3], was applied to study the static and dynamic polarizability of small sodium

* Permanent address now: Departamento de Fisica da Universidade, 3000 Coimbra Portugal.
** Permanent address now: Fritz-Haber Institut der Max-Planck Gesellschaft, Faradayweg 4–6, W-1000 Berlin 33, Germany.

particles [4]. The polarizability is of great interest due to its simple relation to an experimental observable, the photoabsorption cross-section. In short (and at the risk of oversimplification), three main conclusions were drawn then:

1. Quantum Size Effects (QSE) lead to a sizeable red-shift of the plasmon resonance with respect to the classical Mie value.
2. As the cluster size decreases, the volume plasmon gradually disappears.
3. The surface plasmon, which for large clusters displays a single, collective peak, becomes strongly fragmented for the smaller clusters, due to its coupling to electron-hole pair excitations (Landau fragmentation).

Measurements of absolute photoabsorption cross-sections in free clusters were pioneered in Berkeley, in 1987, by de Heer et al. [5]. Since then, many experiments [6] have widened our knowledge of the response of these small systems to light, both in neutral and in positively ionized species.

Theoretically, essentially two microscopic approaches have been used to calculate the photoabsorption cross-section of small metal particles:

1. Ab-initio, all-electron quantum molecular methods [7, 8];
2. Jellium-based TDLDA and related methods [4, 9, 10, 11].

Because metal clusters can be produced with any number of atoms, from the simple dimer to a macroscopic piece of bulk solid, the transition from atomic to bulk behaviour constitutes one of central and most callenging issues to be addressed in this field. In this context, the enormous complexity of the quantum molecular methods, together with their remarkable sensitivity to different basis sets, precludes their practical application. In fact, only few calculations [7] are available which make use of these methods. Irrespective of these drawbacks, the quantum molecular methods are, at least conceptually, capable of producing accurate results for the smallest sizes, being therefore useful as a testing ground for simpler and more flexible many-electron cluster theories.

Jellium-based calculations of the photoabsorption cross-section of small metal particles are now available for a size range spanning over three orders of magnitude [10], but the larger sizes calculated so far ($N \approx 2000$) are still insufficient for the observation of the expected transition to the bulk-live behaviour, which is conjectured to occur for particles containing $\approx 10^4$ atoms [11]. On the other hand, there is experimental evidence for the occurrence of "atomic shells", which are attributed to the dominant effect of faceting in large clusters as compared to the small ones, in which the electronic shells seem to dominate [12]. Clearly, the jellium is a model for electronic shells. Comparison with experiment should, in principle, enable one to infer the relative importance of the atomic structure in the resulting cross-sections by testing the validity of a pure electronic shell model such as the jellium model. To this end, however, one must use an appropriate electronic shell model, since otherwise any conclusions regarding the relative roles played by the electrons and the ions may be hidden in subtle cancellations or wrong assumptions.

In this paper, we address this issue by calculating the photoabsorption cross-section of small metal clusters, within a purely electronic shell model (the jellium model), treating the valence electrons in DFT making use of the LDA for XC. Furthermore, we correct this theory for its most important drawback, as far as small systems are concerned — its self interacting character. The Self-Interaction Correction (SIC) will be carried out in the way proposed by Perdew and Zunger [14] for the calculation of the ground-state properties, which constitutes the most tested and successful of SIC approximations. Furthermore, we shall extend the SIC scheme also to the calculation of the excitation spectrum. To this end we shall correct for self-interaction also in the screening self-

consistent field induced, in linear response theory, by an external perturbation. We believe that the general SIC formulation introduced in the present work provides a state of the art description of excitations in general, finite many-electron systems. By comparing with the available experimental data, we shall infer the importance of the ionic structure, whereas comparison with the standard TDLDA results will enable us to deduce the magnitude of the self-interaction corrections.

Experimental data on alkali metal clusters are by now sufficient to indicate, in short, that the jellium-based LDA and TDLDA approaches are off by as much as 15% in the description of the ground state and excited state properties of these systems, though able to qualitatively reproduce their main features. Many reasons have been invoked to explain this disagreement, the most popular being that a purely electronic shell model is inadequate because it neglects the ionic structure which should play an important role. This line of reasoning prompted a profusion of models [15, 16, 17] which tried to go beyond the jellium model in some more or less phenomenological way, simulating the structure of the ionic cores. In most of these attempts it was required that the resulting model be simple. In our opinion, these procedures may be justifiable only after the electronic part (which constitutes an essential ingredient in all these models) has been worked out in a physically appropriate way. As a matter of fact, we shall obtain results for the static polarizabilities and photoabsorption cross-sections which compare quantitatively with the available experimental data. This indicates that, for the clusters we are considering here, electronic effects play a dominant role, the ionic structure providing a perturbative effect responsible, e.g., for fine (but important) effects in the photoabsorption line shape [18]. This is also supported, at present by three other independent sources of information:

1. As early as 1986, P. Sheng et al. [21] calculated the static polarizabilities of small sodium particles by including elastic deformations in the jellium background. As a result, the polarizabilities were changed by as much as 1%, which is manifestly insufficient to bridge the 15% gap between LDA theory (considered in that paper) and experiment.
2. The recent calculations of U. Röthlisberger and W. Andreoni [20, 22] who performed ab-initio LDA calculations of small (up to 20) neutral sodium clusters, fully relaxing the ionic positions within the Car-Parrinello method, show that angular momentum is approximately a good quantum number to classify the electronic orbitals of the valence electrons of the magic clusters. Furthermore, the densities obtained with the ab-initio method, when sphericalized, become very similar to the densities emerging from the jellium model. Finally, good (even quantitative) agreement was found between the Kohn-Sham eigenvalues of the ab-initio fully relaxed structures and the self-consistent spheroidal jellium model results of Ekardt and Penzar [19, 23].
3. Most important, the experimental determination of the quasiparticle energies of small potassium clusters [25] show striking similarities to the calculated single-particle spectrum of the electronic shell model of Clemenger [26].

This bulk of information leads us to think that the jellium electronic shell model "works well". This is supported by the results of the present work.

The paper is organized as follows. In section 2 the formalism is developed, and its derivation is carried out in close relation with the standard TDLDA. Section 3 is devoted to the discussion of the results and their physical implications, while the general conclusions and future prospects are collected in section 4. Mathematical details are deferred to an appendix.

2 Formalism

To describe the Ground State (GS) of a cluster with $\mathcal{N}$ ions and N valence electrons, in the LDA to XC, we start by solving the Kohn-Sham equations,

$$\left[\frac{-\hbar^2}{2m}\Delta + V_{\mathrm{MF}}(\mathbf{r})\right]\psi_j(\mathbf{r}) = \varepsilon_j\,\psi_j(\mathbf{r})\,, \tag{1}$$

where the LDA mean-field (MF) potentials reads

$$V_{\mathrm{MF}}(\mathbf{r}) = V_{\mathrm{I}}(\mathbf{r}) + e^2\int\frac{n(\mathbf{r}_1)d\mathbf{r}_1}{|\mathbf{r}-\mathbf{r}_1|} + V_{xc}[n(\mathbf{r})],\; n(\mathbf{r}) = \sum_{j=1}^{N}|\psi_j(\mathbf{r})|^2. \tag{2}$$

$V_{\mathrm{I}}(\mathbf{r})$ is the jellium potential of $\mathcal{N}$ positive ions, $\psi_j(\mathbf{r})$ represents the eigenfunction with quantum numbers j, and ε_j is the corresponding eigenvalue. V_{xc} is the LDA for XC for which we use the parametrization of Gunnarsson and Lundqvist [27]. As is clear from the above definition of the average potential, each electron interacts with itself spuriously via the construction of the total electronic potential by means of the total density. The SIC attempts to correct for this deficiency in the average potential, by replacing the above scheme by a similar one, in which a set of Kohn-Sham-like equations is still solved, but now with an orbital dependent potential:

$$\left[\frac{-\hbar^2}{2m}\Delta + \tilde{V}^{(i)}_{\mathrm{SIC}}(\mathbf{r})\right]\tilde{\psi}^{(i)}_j(\mathbf{r}) = \tilde{\varepsilon}^{(i)}_j\,\tilde{\psi}^{(i)}_j(\mathbf{r}), \tag{3}$$

where $\tilde{V}^{(i)}_{\mathrm{SIC}}$ is relate to V_{MF} by

$$\tilde{V}^{(i)}_{\mathrm{SIC}}(\mathbf{r}) = V_{\mathrm{MF}}(\mathbf{r}) - e^2\int\frac{\tilde{n}_i(\mathbf{r}_1)d\mathbf{r}_1}{|\mathbf{r}-\mathbf{r}_1|} - V_{xc}[\tilde{n}_i(\mathbf{r})],\; \tilde{n}_i(\mathbf{r}) = |\tilde{\psi}^{(i)}_i(\mathbf{r})|^2. \tag{4}$$

To make the notation unambiguous, we redefined the eigenfunctions and eigenvalues, such that $\tilde{\psi}^{(i)}_j(\mathbf{r})$ represents the eigenfunction of orbital potential $\tilde{V}^{(i)}_{\mathrm{SIC}}$ with quantum numbers j, and $\tilde{\varepsilon}^{(i)}_j$ the corresponding eigenvalue. Furthermore, we shall consistently denote by X a given self-interacting quantity and by $\tilde{X}$ the corresponding quantity in the SIC case. In this notation the total density appearing in V_{MF} is now defined as [28]

$$\tilde{n}(\mathbf{r}) = \sum_{i=1}^{N}|\tilde{\psi}^{(i)}_i(\mathbf{r})|^2. \tag{5}$$

Contrary to the self-interacting case, in which the Kohn-Sham eigenvalues and eigenfunctions have no direct relation to the quasiparticle energies and wave functions of the cluster, the SIC-LDA solutions are expected to constitute good representations of these quantities (cf. Refs. [14, 29]).

We shall consider now the general theory of linear response to an external perturbation. For definiteness, we shall start with the self-interacting case (TDLDA), including the SIC later.

Under the action of an external, time-dependent perturbation of the form

$$V_{\mathrm{ext}}(\mathbf{r}) = -\,r^l\,P_l(\cos\theta)\cos(\omega t)\,, \tag{6}$$

the valence electrons will respond, to zero order, independently. The independent-particle induced density will oscillate in phase with the external perturbation, its single Fourier component being given by

$$\delta n_0(\mathbf{r}, \omega) = \int d\mathbf{r}_1 \, \chi_0(\mathbf{r}, \mathbf{r}_1; \omega) \, V_{\text{ext}}(\mathbf{r}_1, \omega) \, , \tag{7}$$

where the independent-particle susceptibility is given by

$$\chi_0(\mathbf{r}, \mathbf{r}_1; \omega) = \sum_{i,j=1}^{\infty} (f_i - f_j) \frac{\psi_i^*(\mathbf{r}) \, \psi_j^*(\mathbf{r}_1) \, \psi_j(\mathbf{r}) \, \psi_i(\mathbf{r}_1)}{\hbar\omega - (\varepsilon_i - \varepsilon_j) + i\delta} \tag{8}$$

$$= \sum_{i}^{occ} \psi_i^*(\mathbf{r}) \psi_i(\mathbf{r}_1) G(\mathbf{r}, \mathbf{r}_1, \varepsilon_i + \hbar\omega) + \psi_i(\mathbf{r}) \psi_i^*(\mathbf{r}_1) G^*(\mathbf{r}, \mathbf{r}_1, \varepsilon_i - \hbar\omega) \, . \tag{9}$$

In the above equation, f_i represents the Fermi occupation factor (1 for occupied orbitals and 0 otherwise) and G is the retarded Green's function associated with the LDA Schödinger-type equation,

$$\left[E + \frac{\hbar^2}{2m} \Delta - V_{\text{MF}}(\mathbf{r}) \right] G(\mathbf{r}, r_1, E) = \delta(\mathbf{r} - \mathbf{r}_1) \, ; \tag{10}$$

it possesses the eigenfunction expansion,

$$G(\mathbf{r}, \mathbf{r}_1, E) = \sum_{j=1}^{\infty} \frac{\psi_j(\mathbf{r}) \, \psi_j(\mathbf{r}_1)^*}{E - \varepsilon_j + i\delta} \, . \tag{11}$$

The imaginary infinitesimal δ [31] ensures the appropriate causality properties of this Green's function, fixing the boundary conditions to be imposed on the solution of Eq. (10).

The equality between Eqs. (8) and (9) relies on a subtle cancellation of two terms. Indeed, as becomes clear by simple inspection of Eq. (11), the first term in Eq. (9) includes all transitions from a given occupied state into all possible states (including eventually itself), which manifestly violates the Pauli principle. The Pauli forbidden transitions are exactly cancelled, however, by the second term in Eq. (9). This has the clear advantage that the infinite sums in Eq. (8) are now replaced by a sum over the (finite) occupied, single particle states already determined in the GS calculation, together with the solution of Eq. (10) for the Green's function.

The independent-particle approximation overestimates the response of the system to the external perturbation. This is because the screening electronic field due to the induced density is not taken into account. In linear response, one includes this field by requiring a self-consistency condition between the induced density and the screening potential. Denoting the linearly induced density by δn and expanding the potential in Eq. (2) keeping only the linear terms we get [32]

$$V_{\text{screen}}(\mathbf{r}, \omega) = e^2 \int \frac{\delta n(\mathbf{r}_1, \omega) d\mathbf{r}_1}{|\mathbf{r} - \mathbf{r}_1|} + \frac{\delta V_{xc}[n(\mathbf{r})]}{\delta n} \delta n(\mathbf{r}, \omega) \, . \tag{12}$$

The linear response equation for δn reads, then,

$$\delta n(\mathbf{r}, \omega) = \int d\mathbf{r}_1 \chi_0(\mathbf{r}, \mathbf{r}_1; \omega)[V_{\text{ext}}(\mathbf{r}_1, \omega) + V_{\text{screen}}(\mathbf{r}_1, \omega)] . \tag{13}$$

This equation constitutes the TDLDA equation for the induced density. We proceed now by correcting this formulation including SIC. We shall distinguish two different levels of SIC.

The SIC scheme implies several modifications in the independent-particle response. Since the single-particle potentials are now orbital dependent, the independent-particle susceptibility is conveniently rewritten as

$$\begin{aligned}\tilde{\chi}_0(\mathbf{r}, \mathbf{r}_1; \omega) = & \sum_i^{occ} \tilde{\psi}_i^{(i)*}(\mathbf{r})\, \tilde{\psi}_i^{(i)}(\mathbf{r}_1)\, \tilde{G}^{(i)}(\mathbf{r}, \mathbf{r}_1, \tilde{\varepsilon}_i^{(i)} + \hbar\omega) \\ & + \sum_i^{occ} \tilde{\psi}_i^{(i)}(\mathbf{r})\, \tilde{\psi}_i^{(i)*}(\mathbf{r}_1)\, \tilde{G}^{(i)*}(\mathbf{r}, \mathbf{r}_1, \tilde{\varepsilon}_i^{(i)} - \hbar\omega) \\ = & \sum_i^{occ} \tilde{\Lambda}^{(i)}(\mathbf{r}, \mathbf{r}_1, \omega) .\end{aligned} \tag{14}$$

The (orbital dependent) Green's functions $\tilde{G}^{(i)}$ are now related to the solution of the following equation,

$$\left[E + \frac{\hbar^2}{2m}\Delta - \tilde{V}_{\text{SIC}}^{(i)}(\mathbf{r})\right] \hat{G}^{(i)}(\mathbf{r}, \mathbf{r}_1, E) = \delta(\mathbf{r} - \mathbf{r}_1) , \tag{15}$$

by

$$\tilde{G}^{(i)}(\mathbf{r}, \mathbf{r}_1, \tilde{\varepsilon}_i^{(i)} + \hbar\omega) = \left[\hat{G}^{(i)}(\mathbf{r}, \mathbf{r}_1, \tilde{\varepsilon}_i^{(i)} + \hbar\omega) - \sum_j^{occ} \frac{\tilde{\psi}_j^{(i)}(\mathbf{r})\, \tilde{\psi}_j^{(i)*}(\mathbf{r}_1)}{\tilde{\varepsilon}_i^{(i)} + \hbar\omega - \tilde{\varepsilon}_j^{(i)} + i\delta}\right] . \tag{16}$$

The physics associated with the above equations is quite simple. Because the potential is orbital dependent, the transitions from a given occupied state should be computed with the potential appropriate for this state. This is accomplished through Eq. (15) and ensures that orbitals into which the electron is promoted are SIC as well. The present approach is closely related to the well known Improved Virtual Orbitals (IVO) method widely used in atomic physics and quantum chemistry [34]. $\tilde{G}^{(i)}$ is obtained from $\hat{G}^{(i)}$ through Eq. (16). The additional terms explicitly avoid any violation of the Pauli principle, since in the SIC case, the subtle cancellation discussed above in connection with Eqs. (8) and (9) no longer holds, because the forbidden upward transitions are different from the forbidden downward transitions.

So far, we have defined a SIC independent-particle susceptibility. Calculation now of the linearly induced density via Eq. (13) using the screening potential defined in Eq. (12) leads to the first level of SIC response, which we denote by SIC-TDLDA [35]. This formalism contains most of the essential features inherent to a SIC theory and was shown [35, 36] to lead to systematic improvements with respect to the TDLDA, when compared with available experimental data. However, SIC has been neglected in the screening potential, which implies that screening effects are overestimated at the level of SIC-TDLDA. Indeed, from the definition of V_{screen} in Eq. (12) it is clear that there is a spurious self-interaction due to the fact that this potential is calculated with the total

induced density. The appropriate screening term to incorporate in a SIC theory is an orbital dependent screening which reads (cf. Eq. (12) and Ref. [37])

$$\tilde{V}^{(i)}_{\text{screen}}(\mathbf{r}, \omega) = e^2 \int \frac{[\delta\tilde{n}(\mathbf{r}_1, \omega) - \delta\tilde{n}^{(i)}(\mathbf{r}_1, \omega)]\, d\mathbf{r}_1}{|\mathbf{r} - \mathbf{r}_1|} + \frac{\delta V_{xc}[\tilde{n}(\mathbf{r})]}{\delta n} [\delta\tilde{n}(\mathbf{r}, \omega) - \delta\tilde{n}^{(i)}(\mathbf{r}, \omega)] , \tag{17}$$

where $\delta\tilde{n}^{(i)}(\mathbf{r})$ are now the orbital contributions to the total SIC screened induced density

$$\delta\tilde{n}(\mathbf{r}, \omega) = \sum_i^{occ} \delta\tilde{n}^{(i)}(\mathbf{r}, \omega) . \tag{18}$$

Eq. (18) together with Eqs. (14) and (17) enable us to write now a system of coupled equations (as many as the number of occupied orbitals) constituting what we call FULL-SIC-TDLDA equations:

$$\delta\tilde{n}^{(i)}(\mathbf{r}, \omega) = \int d\mathbf{r}_1 \, \tilde{\Lambda}^{(i)}(\mathbf{r}, \mathbf{r}_1, \omega) \, [V_{\text{ext}}(\mathbf{r}_1, \omega) + \tilde{V}^{(i)}_{\text{screen}}(\mathbf{r}_1, \omega)] . \tag{19}$$

The general solution for $\delta\tilde{n}$ is non-trivial, even at the TDLDA level, and has in this case been carried out only for a restricted class of geometries of the jellium background [9, 38, 39]. When the number of valence electrons corresponds to a "magic number", a spherical shape of the jellium background gives the appropriate choice, the N electrons filling completely a given number of spherical electronic shells. It is then convenient to solve the equations derived earlier in spherical coordinates, in which the integration over the angle variables can be obtained in closed form, reducing the problem to the solution of a set of radial equations (details can be found in the appendix). Moreover, for the external field defined in Eq. (6) (with a well defined angular momentum l), the response is diagonal in l and the polarizability of multipolarity l is related to the l-component $\delta\tilde{n}_l(r, \omega)$ by

$$\alpha_l(\omega) = -e^2 \frac{4\pi}{2l + 1} \int_0^{+\infty} dr \, r^{l+2} \, \delta\tilde{n}_l(r, \omega) , \tag{20}$$

the photoabsorption cross-section being simply given in terms of the imaginary part of α as

$$\sigma(\omega) = (4\pi\omega/c) \, Im[\alpha_{l=1}(\omega)] . \tag{21}$$

This equation completes our formalism. Before discussing the results, we would like to comment on the applicability of the general formalism just developed. The SIC proposed in Ref. [14] and adopted in the present work was shown to reduce to the LDA in the limit of extended systems, such as bulk metals. The same features are expected for the SIC of the self-polarization in the original LDA screening potential. In practice, this means that the SIC provides a finite size effect, and as such, it is worth consideration in finite systems, excellent examples of which are atoms, molecules and clusters. For such systems, SIC is expected to provide significant improvements with respect to LDA.

3 Results and discussion

We applied the formalism developed in the previous section to the calculation of static and dynamic dipole polarizabilities (that is, $l = 1$ in Eq. (6)) of sodium particles (this, in our formulation, means that we fix the Wigner-Seitz radius r_s to be that of bulk sodium, 4 a.u.) with 8, 20 and 40 valence electrons, in different ionization states namely, $\{Na_8, Na_9^+\}$, $\{Na_{20}, Na_{21}^+\}$ and $\{Na_{40}, Na_{41}^+\}$. We shall begin by discussing the results obtained for the static polarizabilities, proceeding with the results for the photoabsorption cross-sections.

3.1 Static polarizabilities

Table 1 shows the results for the static dipole polarizability of all clusters considered in this work. The first two columns display the results for the case in which this quantity is computed with Eq. (20), replacing $\delta\tilde{n}_{l=1}(r)$ by its independent-particle counterparts, calculated in LDA ($\delta n_{0,l=1}(r)$) and SIC-LDA ($\delta\tilde{n}_{0,l=1}(r)$) by means of Eq. (13) and neglecting screening effects. The remaining columns correspond to the TDLDA, SIC-TDLDA and FULL-SIC-TDLDA screened polarizabilities, and to the experimental results [41], (available only for the neutral species). Since the LDA eigenfunctions are very good representations of the quasiparticle wave functions [40], the increase in the independent-particle polarizability (from LDA to SIC-LDA) is mainly due to the fact that in SIC-LDA the quasiparticle energies are used, instead of the Kohn-Sham eigenvalues utilized in the LDA case (cf. Eqs. (8) and (14)). As anticipated, the neglect of screening leads to a rough overestimation of the response. Screening effects play a fundamental role at all levels of response, as can be inferred from the remaining columns of Table 1. Both in TDLDA and in SIC-TDLDA, screening leads now to static polarizabilities which are too small. Note, however, that SIC-TDLDA shows a significant and systematic improvement with respect to TDLDA and in better agreement with experiment. By comparing the SIC-TDLDA and FULL-SIC-TDLDA results, one can conclude that the underestimation of the polarizabilities is due to spurious self-interaction in screening. Indeed, both at TDLDA and SIC-TDLDA levels an electron screens itself, which leads to too much screening. By including SIC, excellent agreement with experimental data is obtained.

We would like to point out, finally, that for each group of clusters with a given number of valence electrons, the polarizability is smallest for the cations. This is qualitatively

Table 1 Results for the static polarizabilities of $\{Na_8, Na_9^+\}$, $\{Na_{20}, Na_{21}^+\}$ and $\{Na_{40}, Na_{41}^+\}$, in uits of $\tilde{R}_0^3 = Nr_s^3$ (where N is the number of valence electrons) calculated using the LDA and SIC-LDA independent-particle response (which neglects any screening effects), as well as using the TDLDA, SIC-TDLDA and FULL-SIC-TDLDA screened responses. EXP stands for the experimental values taken from Ref. [41].

	LDA	SIC-LDA	TDLDA	SIC-TDLDA	FULL-SIC-TDLDA	EXP
Na_8	4.95	5.23	1.41	1.52	1.70	1.72 ± 0.03
Na_9^+	4.50	4.69	1.23	1.31	1.46	
Na_{20}	8.00	8.64	1.34	1.46	1.61	1.58 ± 0.04
Na_{21}^+	7.64	8.15	1.24	1.33	1.45	
Na_{40}	11.80	12.70	1.30	1.41	1.51	1.56 ± 0.04
Na_{41}^+	11.49	12.28	1.24	1.32	1.41	

understood in terms of the net confining force with which the ionic background attracts the valence electrons. Because this force is largest in the cations, the electronic density will be most compressed, leading to the smallest polarizability. This qualitative reasoning is fully supported by a straightforward calculation of different radial moments of the associated ground-state densities, which are, of course, smallest for the cations.

3.2 Photoabsorption cross-section

Results for the dynamical response of the 8, 20 and 40 valence electron systems, at all levels of response, are plotted in Figs. 1 to 3, respectively. In each figure, and whenever available, experimental data are illustrated by horizontal arrows indicating the energy range covered experimentally at present, and by vertical arrows positioning the plasmon peaks identified so far.

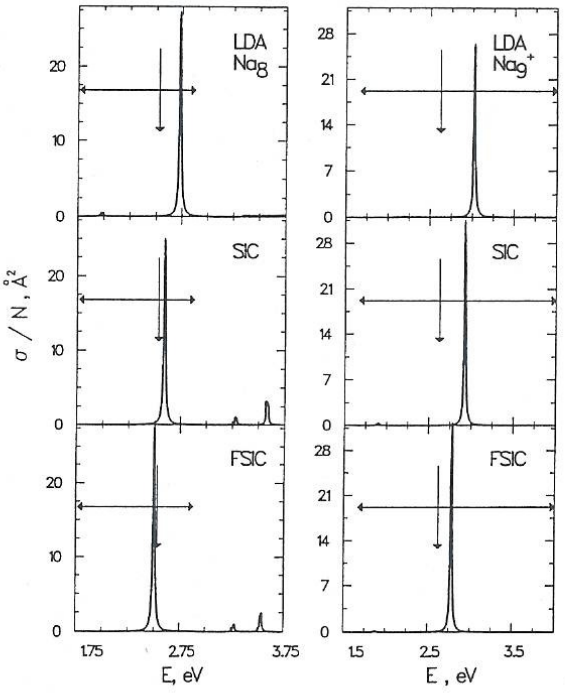

Fig. 1 Line shapes of the photoabsorption cross section per valence electron for Na_8 and Na_9^+, calculated with TDLDA (LDA), SIC-TDLDA (SIC) and FULL-SIC-TDLDA (FSIC). The experimental features are illustrated with arrows. Horizontal arrows display the energy interval spanned by present-day experiments [44, 45, 52], whereas vertical arrows position the peaks which have been resolved experimentally or for which there is tentative evidence.

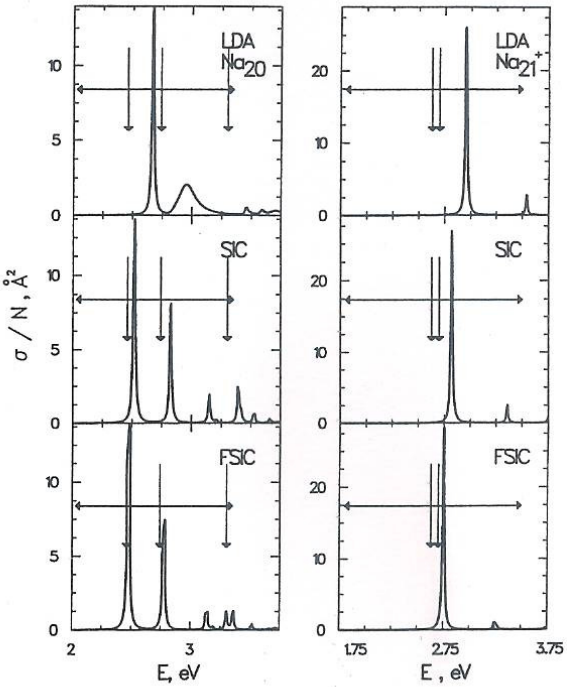

Fig. 2 Same as Fig. 2 for Na_{20} and Na_{21}^+.

Numerical details of the multi-peaked structure of the dynamical response are given in Tab. 2. For each cluster, the position of the main peaks of the cross sections calculated at all levels of response are tabulated, together with the experimental positions resolved up to now. We tried to maintain the correspondence between the different peaks by tabulating them along the same row. In some cases, we thought it more instructive to provide not one single peak position, but a weighted average of several (closely lying)

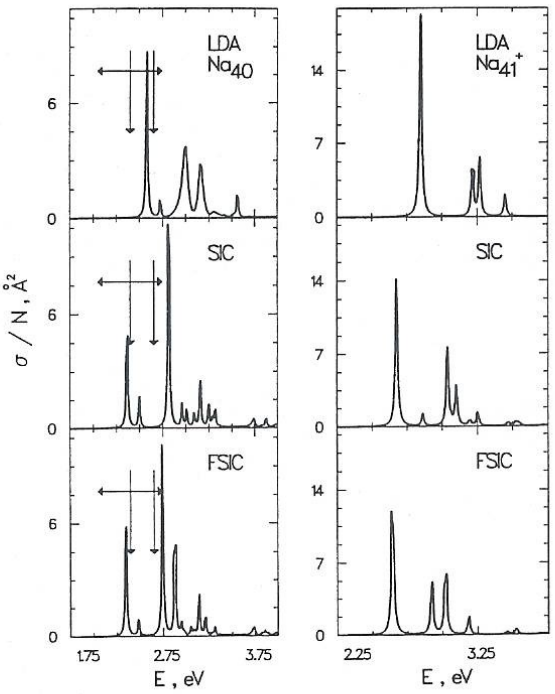

Fig. 3 Same as Fig. 2 for Na_{40} and Na_{41}^+. We would like to point out, however, that the energy window resolved experimentally displays a line shape markedly different from the line shapes obtained for the 8 and 20 valence electron systems. Whereas in these smaller systems the peaks indicated correspond to pronounced humps, the line shape of Na_{40} is rather flat, with the two peaks indicated scarcely emerging from a rather structureless background [44].

peaks, calculated over a small energy interval comprising them. This corresponds to the numbers followed by stars. In this way, the numbers tabulated are semi-quantitative but still illustrative of the detailed features of the different photoabsorption cross sections.

Figs. 1 to 3 display photoabsorption cross-sections which show, in some cases, a multipeaked structure. Because these excitations lie somewhat below the threshold for electron detachment, the quantum size effect leading to the breaking of the strength — Landau fragmentation — is well understood and has been extensively discussed already at the level of TDLDA [4, 10]. The fragmentation is due to the coupling between the surface plasmon and discrete, bound, electron-hole excitations which occur at an excitation energy nearly degenerate with the plasmon energy. This can be easily confirmed by simple inspection of the unscreened cross-section (or, equivalently, the unscreened or independent-particle dynamical polarizability), which has simple poles at the electron-hole excitation energies. Since Landau fragmentation depends sensitively on the quasiparticle excitation energies, it is important to have an accurate and consistent [42] description of these. We would like to mention, in passing, that the classical formula $\omega^2 = \mathrm{Ne}^2/(m\alpha)$ fails to relate the static polarizabilities with the peak positions of the plasmon resonance even in the simplest cases, such as Na_8, Na_9^+ or Na_{21}^+, for which the small amount of Landau fragmentation makes it most likely for the formula to work best (Landau fragmentation, being a pure quantum size effect, is not accounted for by the classical formula). However, as can be inferred from Tables 1 and 2, excellent agreement for the static polarizabilities and peak positions of Na_8 and Na_{20} is obtained with FULL-SIC-TDLDA. This, in turn, indicates that care must be exercised when attributing this failure to an electronic effective mass different from the standard m_e value [16, 46].

Common to all clusters considered here is a progressive red-shift of the whole dynamical response from TDLDA to SIC-TDLDA to FULL-SIC-TDLDA. This systematic feature leads, in turn, to a systematic improvement of the agreement between the theoretical results and the available experimental data. Furthermore, in both SIG responses we observe, mostly for the case of neutral species, an increase of strength in

Table 2 Energy positions (in eV) of the main peaks associated with the dynamical response of {Na_8, Na_9^+}, {Na_{20}, Na_{21}^+} and {Na_{40}, Na_{41}^+}, is given at different levels of response, namely TDLDA (under the column E_{LDA}), SIC-TDLDA (E_{SIC}) and FULL-SIC-TDLDA (E_{FSIC}). The experimentally resolved peaks are given under the column E_{EXP}. The results for the neutral clusters were extracted from Refs. [44, 45], whereas the results for the cationic species were taken from Ref. [52]. Note that the UV part of the spectrum is partially resolved, for Na_{20} in Ref. [45], in which case a small peak at ≈ 3.3 eV cannot be ruled out. We therefore included it in the present table.

	E_{LDA}	E_{SIC}	E_{FSIC}	E_{EXP}
Na_8	2.73	2.59	2.50	2.52
		3.28	3.28	
		3.58	3.54	
Na_9^+	3.02	2.92	2.78	2.62
Na_{20}	2.67	2.52	2.48	2.46
	2.96	2.82	2.78	2.74
	3.46	3.15	3.14	
		3.39*	3.30*	3.30
		3.53	3.36	
		3.66	3.52	
Na_{21}^+				2.63
	2.95	2.82	2.75	2.70
	3.54	3.36	3.25	
		3.80*	3.76*	
Na_{40}	2.58	2.37	2.35	
	2.72	2.50	2.48	2.40
	3.00	2.81	2.74	2.65
	3.16	2.97*	2.89*	
	3.34*	3.14*	3.12*	
	3.6	3.29*	3.26*	
Na_{41}^+	2.85	2.68	2.64	
		2.86		
	3.21	3.03	2.92	
	3.27	3.10	3.02	
	3.45	3.32*	3.19	

the Ultra-Violet (UV) region of the absorption spectrum, at the "expense" of the strength in the visible region. These features can be related with electronic excitations to the loosely bound Rydberg states which are now properly incorporated in the SIC response [35]. For the 40 valence electron clusters, this effect is notorious. Indeed, already at the TDLDA level there is a sizeable accumulation of strength in the UV region, which is poorly described at this level of response. By incorporating the Rydberg states (SIC-TDLDA and FULL-SIC-TDLDA) one observes a fragmentation of the UV strength into a series of small peaks. The strongest peak emerges now at ≈ 2.8 eV, being red-shifted by ≈ 0.2 eV with respect to the corresponding peak in TDLDA (cf. Table 2).

The accumulation of strength in the UV region is smaller in the cationic clusters. This is because the orbital-dependent SIC potentials are considerably deeper than the corresponding ones for the neutral partners, the overlap between the bound states and the Rydberg states being therefore smaller for the cationic clusters.

The UV structure is found already at the SIC-TDLDA level. In general, from SIC-TDLDA to FULL-SIC-TDLDA, important redistributions of strength take place, the larger the number of valence electrons (within the sizes considered here), the more

important the redistributions become. Indeed, while for the 8 valence electron systems one observes similar peak structures with depletion of strength from the UV region into the visible, for the 20 valence electron systems the UV structure is sizeably affected by the SIC in the screening terms. Because for these systems most of the strength lies well below this region, the net effect is a "flattening" of the response, with the UV strength shared among several peaks. However, the SIC-TDLDA and FULL-SIC-TDLDA line shapes are still similar for the 8 and 20 valence electron systems. For the 40 valence electron systems the SIC-TDLDA and FULL-SIC-TDLDA line shapes are markedly different. Whereas the line shape below ≈ 2.8 eV follows the trends already discussed, major changes are observed at higher energies between ≈ 2.8 and ≈ 3.5 eV. For instance, and in this energy region, the three average peaks quoted in Table 2 have, besides distinct features in their line shapes, associated strengths exhausting approximately 6, 10 and 8 percent of the total integrated cross section at the SIC-TDLDA level, whereas they exhaust approximately 19, 8 and 6 percent at the FULL-SIC-TDLDA level. Finally, we would like to point out that the overall red-shift of the response is not equal for different peaks (cf. Table 2).

A direct comparison of the line shape and line width of the photoabsorption cross section calculated in the present work and the experimental observations is not adequate, because of the existence of relaxation mechanisms of the plasmon resonance not accounted for at any level of the linear response formalisms considered here and which are responsible for its finite lifetime, as well as an associated sizeable line width of the photoabsorption cross section. Indeed, the relaxation mechanisms pertinent to the clusters considered in the present work have been explained to arise mostly from the following three mechanisms [47, 38]:

1. Decay of the plasmon into incoherent electronic excitations (Landau fragmentation/damping),
2. scattering of the electron with the phonons of the lattice (resistivity),
3. coupling of the plasmon to quantal and thermal fluctuations of th surface.

The effect of these additional mechanisms (two and three, since mechanism one has already been included) can be simulated, in an average way, by folding the calculated cross-sections with normalized Lorentzian functions, including damping ratios resulting from the couplings mentioned above. If, in entire analogy to what was done in Ref. [35], this procedure is carried out, using the damping ratios obtained in Ref. [47], good agreement is found between the folded FULL-SIC-TDLDA results and experimental data for both Na_8 and Na_{20}. However, for the remaining clusters, the agreement is not so good. This can already be inferred from the schematic comparison carried out in Figs. 1 to 3, from which we believe that useful information can be extracted.

The results of the electronic shell model essentially scale with the Wigner-Seitz radius r_s. This, in turn, leads one to believe that all simple metal clusters will have similar line shapes associated with their photoabsorption profiles. Experiment shows [48] that, in particular for the positively ionized potassium clusters, both K_9^+ and K_{21}^+ have their line shape dominated by one strong peak (which can be very well described with FULL-SIC-TDLDA), in clear contrast with the sodium case considered in the present paper. Therefore, one can expect that the ionic structure will contribute to perturb the purely electronic features described in the present work. In this context, notice that the experimentally observed "lattice shrinkage" effect [49] (for copper clusters) seems to indicate that the bulk value used in the present work for r_s is not realistic. On the other hand, the polarizability measurements of Ref. [41] show no indication of this. Whereas the "lattice shrinkage" effect can be simply understood as a surface-to-volume ratio

effect, this issue remains at present an open and rather disturbing problem. Indeed, we are not aware of any careful study of the variation of the bond length with cluster size and ionization state. It is natural to expect that the bond length between neighbouring Sodium atoms will be different in, e.g., Na_{20} and Na_{21}^+, due to the different net electrostatic balance between electrons and ions, a feature which is not accounted for within the jellium model. This, together with a different overall geometric structure, may lead to different ionic contributions to the single-particle potentials. Preliminary results [50], as well as phenomenological work aiming at mimicking the ionic structure [16, 17], do point in this direction. In particular, we believe that the perturbations caused by the ionic structure will be responsible for the small (≈ 0.07) splitting of the plasmon peak in Na_{21}^+. Moreover, it may act to perturb further the photoresponse of Na_{40}, so as to break up the FULL-SIC-TDLDA peak at 2.74 eV, providing an additional red-shift for part of this peak and also additional flattening of the resulting line shape. Work along these lines is in progress, aiming at introducing a workable, yet predictive theory of the ionic structure [50].

4 Conclusions

A new formulation of linear response theory has been introduced, which includes SIC both in the ground state and in the screened interaction. It has been applied to sodium clusters of different sizes and in different ionization states, namely {Na_8, Na_9^+}, {Na_{20}, Na_{21}^+} and {Na_{40}, Na_{41}^+}. The results, when compared with the previous forms of linear response, show a systematic improvement and, to date, the best overall agreement with the available experimental data, for all clusters considered, without making use of any adjustable parameters. Furthermore, the results of the present work, in particular the difficulties in accounting simultaneously for the features of the neutral and cationic line shapes, enable us to infer the magnitude and type of effects to be expected from the inclusion of the discrete ionic structure, which has been ignored in the present electronic shell model.

Finally, we would like to point out that the formalism developed in this work satisfies basic theorems and properties to be expected from a DFT [14], leading to potentials which display the appropriate asymptotic behaviour [35] expected from general finite, many-electron systems. This opens the possibility to study previously intractable systems (at the level of TDLDA), such as the dynamical response of anions and anionic clusters. Work along these lines is under way.

5 Appendix

In this appendix we list the relevant expressions concerning the solution of the FULL-SIC-TDLDA problem in spherical coordinates.

We write, for the wave functions $\tilde{\psi}_j^{(i)}(\mathbf{r})$,

$$\tilde{\psi}_j^{(i)}(\mathbf{r}) = R_{nj,lj}^{(i)}(r)\, Y_{lj}^{mj}(\hat{r}) \,, \tag{22}$$

where $R_{nj,lj}^{(i)}(r)$ are the solutions of the radial version of Eq. (3) and $Y_{lj}^{mj}(\hat{r})$ are the usual spherical harmonics. As usual, and due to the fact that all orbitals are fully occupied, the density $\tilde{n}(\mathbf{r})$ depends only on the radial coordinate, the same happening with the potential $\tilde{V}_{\mathrm{SIC}}(\mathbf{r})$ in Eq. (3). We consider also the spherical harmonic decomposition of $\tilde{G}(\mathbf{r}, \mathbf{r}_1, E)$ and $\tilde{\chi}_0(\mathbf{r}, \mathbf{r}_1; \omega)$ which, due to the rotational invariance of the system, can be written:

$$\tilde{G}(\mathbf{r}, \mathbf{r}_1, E) = \sum_l Y_l^*(\hat{r})\, \tilde{G}_l(r, r_1, E)\, Y_l(\hat{r}_1) ,$$

$$\tilde{\chi}_0(\mathbf{r}, \mathbf{r}_1, \omega) = \sum_l Y_l^*(\hat{r})\, \tilde{\chi}_{0l}(r, r_1, \omega)\, Y_l(\hat{r}_1) .$$

Eq. (15) may be written in the form

$$\left[E + \frac{1}{r^2}\frac{\partial}{\partial r} r^2 \frac{\partial}{\partial r} - \frac{l(l+1)}{r^2} - \tilde{V}^{(i)}_{\mathrm{SIC}}(r)\right] \hat{G}_l(r, r_1, E) = \frac{\delta(r - r_1)}{r^2} . \quad (23)$$

The sign of the imaginary part in Eq. (11) determines the boundary conditions to be imposed on the solution of the above equation. Denoting by $j_l(r, E)$ the solution of the homogeneous version of the above equation which is regular at the origin and denoting by $h_l(r, E)$ the solution which behaves asymptotically as an outgoing wave, we can construct the Green's function in the following way [51]:

$$\hat{G}_l(r, r_1, E) = \frac{j_l(r_<, E) h_l(r_>, E)}{[r^2[j_l(r)\, h_l'(r) - j_l'(r)\, h_l(r)]]_{r=a}} , \quad (24)$$

where a is an arbitrary constant (in the sense that the denominator (Wronskian) is independent of a), $r_<$ and $r_>$ being, respectively, the smaller and larger of $\{r, r_1\}$.

The spherical harmonic decomposition of $\tilde{\chi}_0(\mathbf{r}, \mathbf{r}_1, \omega)$ leads to the following expression for its l-component:

$$\begin{aligned}\tilde{\chi}_{0l}(r, r_1, \omega) &= \sum_i^{occ} \tilde{\Lambda}_l^{(i)}(r, r_1, \omega) \\ &= \sum_i^{occ} \frac{2l_i + 1}{2\pi} R^{(i)}_{n_i, l_i}(r)\, R^{(i)}_{n_i, l_i}(r_1) \sum_{k=0}^{\min[l, l_i]} \frac{a_{l-k} a_k a_{l_i - k}}{a_{l_i + l - k}} \frac{2l_i + 2l - 4k + 1}{2l_i + 2l - 2k + 1} \\ &\quad \times [\tilde{G}_{l_i + l - 2k}(r, r_1, \varepsilon^{(i)}_{n_i, l_i} + \omega) + c.c.[\omega \to -\omega]] . \end{aligned} \quad (25)$$

In the above equation, $a_k = (2k - 1)!!/k!$. For a given external perturbation of multipolarity l as defined in Eq. (6), and once the $\tilde{\Lambda}_l^{(i)}(r, r_1, \omega)$ have been constructed, the linearly induced density is given by the solution of the following set of equations,

$$\delta\tilde{n}_l^{(i)}(r, \omega) = \int_0^\infty dr_1 r_1^2\, \tilde{\Lambda}_l^{(i)}(r, r_1, \omega)[r^l + \tilde{V}^{(i)}_{\mathrm{screen}}(r_1, \omega)] , \quad (26)$$

where $\tilde{V}^{(i)}_{\mathrm{screen}}(r_1, \omega)$ reads

$$\begin{aligned}\tilde{V}^{(i)}_{\mathrm{screen}}(r_1, \omega) &= \frac{\partial V_{xc}[n(r_1)]}{\partial n} [\delta\tilde{n}(r_1\, \omega) - \delta\tilde{n}^{(i)}(r_1, \omega)] \\ &\quad + \frac{4\pi e^2}{2l + 1} \int_0^\infty dr_2 r_2^2 \frac{r_<^l}{r_>^{l+1}} [\delta\tilde{n}(r_2, \omega) - \delta\tilde{n}^{(i)}(r_2, \omega)] . \end{aligned}$$

There are as many equations as occupied orbitals, which are coupled via the definition of $\delta\tilde{n}(\mathbf{r}, \omega)$, Eq. (18).

References

[1] W. Ekardt, Phys. Rev. **B29** (1984) 1558

[2] W. D. Knight et al., Phys. Rev. Lett. **52** (1984) 2141

[3] M. J. Stott, E. Zaremba, Phys. Rev. **A21** (1980) 12; Phys. Rev. **A22** (1980) 2293; A. Zangwill, P. Soven, Phys. Rev. **B21** (1980) 1561; G. D. Mahan, Phys. Rev. **A22** (1980) 1780

[4] W. Ekardt, Phys. Rev. Lett. **52** (1984) 1925; Phys. Rev. **B31** (1985) 6360

[5] W. de Heer et al., Phys. Rev. Lett. **59** (1987) 1805

[6] Risking some serious omissions, this is an attempt at a representative view of recent experiments: K. Selby et al., Phys. Rev. **B40** (1989) 5417; C. R. C. Wang et al., Z. Phys. **D19** (1991) 13; H. Fallgren, T. P. Martin, Chem. Phys. Lett. **168** (1990) 233; C. Bréchignac et al., Chem. Phys. Lett. **164** (1989) 433; J. Blanc et al., Z. Phys. **D19** (1991) 7; K. Selby et al., Phys. Rev. **B43** (1991) 4565; J. Tiggesbäumker et al., to be published

[7] V. B. Koutecký et al., Chem. Rev. **91** (1991) 1035 and references therein by the same group

[8] In the quantum-molecular methods [7] optical excitations are computed including electron correlations within a truncated part of the subspace including *double-pair* electron-hole excitations. This is formally different from the TDLDA approach which considers, besides the electron correlation effects already included in the exchange-correlation functional, the correlations obtained by including the full subspace of *single-pair* electron-hole excitations

[9] References in this entry by no means exhaust the whole bulk of calculations available at present. W. Ekardt, Phys. Rev. **B32** (1985) 1961; D. E. Beck, Phys. Rev. **B30** (1984) 6935; Phys. Rev. **B35** (1987) 7325; Phys. Rev. **B43** (1991) 7301; M. J. Puska et al., Phys. Rev. **B31** (1985) 3486; Phys. Rev. **B33** (1985) 4289; M. Brack, Phys. Rev. **B39** (1989) 3533; C. Yannouleas et al., Phys. Rev. Lett. **B63** (1989) 255; Phys. Rev. **B41** (1990) 6088; Phys. Rev. **A44** (1991) 5901; R. A. Broglia et al., Phys. Rev. **B44** (1991) 5901; S. Saito et al., Phys. Rev. **B42** (1990) 7391

[10] C. Yannouleas, R. A. Broglia, "Landau Damping and Wall Dissipation in Large Metal Clusters", preprint

[11] W. Ekardt, J. M. Pacheco, to be published

[12] This, in turn may be a temperature dependent effect. Indeed, preliminary experimental results do not rule out that electronic shell structure may dominate at high temperatures, whereas atomic shells may interfere at low temperatures [13]

[13] T. P. Martin et al., Chem. Phys. Lett. **186** (1991) 53

[14] J. P. Perdew, A. Zunger, Phys. Rev. **B23** (1981) 5048

[15] M. Iñiguez et al., Z. Phys. **D11** (1989) 163

[16] C. Yannouleas, R. A. Broglia, Europhys. Lett. **15** (1991) 843

[17] A. Rubio et al., to be published

[18] Similar trends are expected in deformed clusters [19, 20], this case being presently under study

[19] W. Ekardt, Z. Penzar, Phys. Rev. **B38** (1988) 4273

[20] U. Röthlisberger, W. Andreoni, J. Chem. Phys. **94** (1991) 8129; contribution to the 88. WE-Heraeus-Seminar on "Nuclear Physics Concepts in Atomic and Cluster Physics", Bad-Honef, Germany, November 1991

[21] P. Sheng et al., Phys. Rev. **B34** (1986) 732

[22] We would like to point out that these LDA, self-interacting calculations show excellent agreement for the fully relaxed structures with the results of the quantum molecular calculations [7] for the smallest sizes. However, unresolved discrepancies between the geometrical structures obtained with the 2 methods persist for the larger sizes

[23] Both calculations were performed within the LDA neglecting SIC. SIC was later incorporated in the self-consistent spheroidal jellium model of Ref. [19] to calculate gound state properties of small metallic clusters [24]

[24] Z. Penzar, W. Ekardt, Z. Phys. **D17** (1990) 69

[25] Contribution of K. Bowen to the 88. WE-Heraeus-Seminar on "Nuclear Physics Concepts in Atomic and Cluster Physics", Bad-Honef, Germany, November 1991

[26] K. Clemenger, Phys. Rev. **B32** (1985) 1359

[27] O. Gunnarsson, B. I. Lundqvist, Phys. Rev. **B13** (1976) 4274

[28] The SIC corrections lead to an orbital dependent potential, which in turn leads to eigenfunctions which are not orthogonal. This problem is easily overcome by orthonormalizing the wave functions at each cycle of the self-consistent iteration scheme, and was adopted in all calculations reported in this paper

[29] Indirect support is provided by the calculation of the quasiparticle energies of small sodium and potassium clusters in the so-called GW approximation [30]. The results of this approximation lead to quasiparticle energies and wave functions in good agreement with our ground-state results
[30] S. Saito et al., Phys. Rev. **B 40** (1989) 3643; J. Phys.: Condens. Matter **2** (1990) 9041
[31] In all numerical calculations carried out in this paper, δ was given a numerical value of 10 meV, to avoid divergences at the poles of the Green's functions. This "numerical damping" is responsible for the very small line width displayed by the photoabsorption peaks of Figs. 1 to 3
[32] In general, the functional derivative in Eq. (12) leads to a non-local term in the screening potential. We keep the standard approximation of replacing this term by the local term $\partial V_{xc}[n(\mathbf{r})]/\partial n\, \delta n(\mathbf{r})$. Furthermore we neglect any time dependence in this term (static approximation). This has been estimated to constitute a very good approximation [33]
[33] E. K. U. Gross, W. Kohn, Phys. Rev. Lett. **55** (1985) 2850
[34] W. J. Hunt, W. A. Goddard, Chem. Phys. Lett. **3** (1969) 414
[35] J. M. Pacheco, W. Ekardt, to be published
[36] J. M. Pacheco, W. Ekardt, in: Physics and Chemistry of Finite Systems: From Clusters to Crystals, to be published in NATO Advanced Study Institute Series B: Physics, P. Jena, B. K. Rao, S. N. Khanna (eds.), Plenum Press, New York 1991
[37] P. Stampfli, K. H. Bennemann, in: Physics and Chemistry of Small Clusters, vol. 158 of NATO Advanced Study Institute Series B: Physics, P. Jena, B. K. Rao, S. N. Khanna (eds.), Plenum, New York 1987, p. 473
[38] W. Ekardt, Z. Penzar, Phys. Rev. **B 43** (1991) 1322
[39] M. Bernath et al., Phys. Lett. **156** (1991) 307
[40] Indeed, it was already found in Ref. [30] that the overlap between the quasiparticle wave functions (calculated in the GW approximation) and the LDA Kohn-Sham eigenfunctions is in all cases very close to 1. Similar results are obtained (as expected), when SIC is performed on LDA
[41] W. D. Knight et al., Phys. Rev. **B 31** (1985) 2539
[42] We would like to stress that it is very important to carry out the SIC correction consistently. As an example, note that the authors of Ref. [43] computed photoabsorption cross-sections in an approximate SIC response formalism in which all orbitals are SIC in the same way. This, in turn, leads to a poor description of the quasiparticle energies (we checked that this scheme leads to unsystematic deviations of as much as 0.5 eV between their quasiparticle energies and ours — or for that sake, the ones obtained with the GW approximation [30]) and to cross-sections for the magic clusters with many isolated peaks, which is not supported by the available experimental data [44, 45]
[43] S. Saito et al., Phys. Rev. **B 43** (1991) 6804
[44] K. Selby et al., (1991) in Ref. [6]
[45] S. Pollack et al., J. Chem. Phys. **94** (1991) 2496
[46] J. Blanc et al., J. Chem. Phys., in press
[47] J. M. Pacheco, R. A. Broglia, Phys. Rev. Lett. **62** (1980) 1400; G. F. Bertsch, D. Tománek, Phys. Rev. **B 40** (1989) 2749; C. Yannouleas et al., Phys. Rev. **B 41** (1990) 6088; J. M. Pacheco et al., Z. Phys. D 21 (1991) 289
[48] C. Bréchignac et al., Chem. Phys. Lett. **164** (1989) 433
[49] G. Apai et al., Phys. Rev. Lett. **43** (1979) 165
[50] W. D. Schöne, W. Ekardt, J. M. Pacheco, in preparation
[51] See, for example, G. Arfken, Mathematical methods for Physicists, 3rd ed., Academic Press, 1985
[52] C. Bréchignac et al., Chem. Phys. Lett (in press)